The shape of a Möbius band

By L. Mahadevan and Joseph B. Keller

Departments of Mathematics and Mechanical Engineering, Stanford University, Stanford, California 94305, U.S.A.

The shape of a Möbius band made of a flexible material, such as paper, is determined. The band is represented as a bent, twisted elastic rod with a rectangular cross-section. Its mechanical equilibrium is governed by the Kirchhoff–Love equations for the large deflections of elastic rods. These are solved numerically for various values of the aspect ratio of the cross-section, and an asymptotic solution is found for large values of this ratio. The resulting shape is shown to agree well with that of a band made from a strip of plastic.

1. Introduction

Invented by the German mathematician F. A. Möbius in 1858, the eponymous Möbius band is the canonical example of a one-sided surface or non-orientable 2-manifold. A physical model of it can be made from a sufficiently long rectangular strip of paper by twisting one end through 180° and then gluing it to the other end. Such models always have a characteristic shape. Our goal is to determine this shape in terms of the dimensions of the strip and the elastic properties of the material of which it is made.

Sadowsky (1930) first attempted to do this by formulating an energy minimization problem for the band represented as an inextensible elastic shell. Although he did not succeed, he did find an upper bound on the minimum energy by choosing a trial shape. Later, Wunderlich (1963) was able to lower this upper bound by choosing a different trial shape. This early work and related geometric aspects of Möbius bands are described by Schwarz (1990).

Instead of following Sadowsky, we model the Möbius band as an elastic rod with a rectangular cross-section. Its ends are joined together after undergoing one half-twist relative to each other, and at equilibrium no external forces or torques act on it. This equilibrium configuration is determined by the equations of the Kirchoff–Love theory for the large deflections of bent and twisted elastic rods. When supplemented by the appropriate kinematic relations, they lead to a twelfth order system of ordinary differential equations with six boundary conditions at each end of the rod.

This two-point boundary-value problem is formulated in §2. In §3 it is made dimensionless and the two-fold symmetry of the band about a certain axis is used to halve the interval over which the problem must be solved. An exact solution of the problem for a rod with a square cross-section is presented in §4, together with a numerical method for solving the problem for any aspect ratio of the cross-section. It uses continuation with respect to the aspect ratio, and utilizes the exact solution as its starting point. Graphs of the numerical results for various values of the aspect ratio are presented. An asymptotic solution for large values of this aspect ratio is

Proc. R. Soc. Lond. A (1993) **440**, 149–162
Printed in Great Britain

determined in §5, and it is shown to be in good agreement with the results for large finite aspect ratios. In §6, the elastic energy of the asymptotic solution is calculated. The inextensible shell model is considered in §7. A method for the construction of a developable surface associated with the asymptotic solution is given and an upper bound on the energy of an equilibrated Möbius band is computed. It is seen to be a considerable improvement on the bounds in Sadowsky (1930) and Wunderlich (1963).

2. Formulation

We consider the equilibrium of a thin elastic rod subjected to no external forces or couples. The balance of net forces and couples at every cross-section of such a rod gives the six equations (Love 1927, pp. 387–388)

$$N_s^{(1)} - N^{(2)}\tau + T\kappa^{(2)} = 0, \tag{2.1}$$

$$N_s^{(2)} - T\kappa^{(1)} + N^{(1)}\tau = 0, \tag{2.2}$$

$$T_s + N^{(2)}\kappa^{(1)} - N^{(1)}\kappa^{(2)} = 0, \tag{2.3}$$

$$G_s^{(1)} - G^{(2)}\tau + H\kappa^{(2)} - N^{(2)} = 0, \tag{2.4}$$

$$G_s^{(2)} - H\kappa^{(1)} + G^{(1)}\tau + N^{(1)} = 0, \tag{2.5}$$

$$H_s - G^{(1)}\kappa^{(2)} + G^{(2)}\kappa^{(1)} = 0. \tag{2.6}$$

Here s is the arc-length along the centre line of the rod, $N^{(1)}(s)$ and $N^{(2)}(s)$ are the components of the shearing force along the principal axes, $T(s)$ is the tension, $G^{(1)}(s)$ and $G^{(2)}(s)$ are the components of the flexural couple along the principal axes, $H(s)$ is the torsional couple, $\kappa^{(1)}(s)$ and $\kappa^{(2)}(s)$ are the components of the curvature of the centre line along the principal axes and $\tau(s)$ is the twist of the rod. The principal axes of the rod at the point s along it are oriented along the orthogonal directions about which the moments of inertia of the normal cross-section achieve their maximum and minimum values. Note that these equations are valid in a reference frame which is convected along the centre line at unit velocity; this frame is aligned with the orthogonal triad consisting of the tangent to the centre line and the principal axes of the rod at every point along it.

The ordinary approximate theory of a naturally straight thin rod is a generalization of Euler–Bernoulli beam theory. In it, it is assumed that the stress-couples are connected to the curvature and the twist by the equations (Love 1927, p. 389)

$$G^{(1)} = EI^{(1)}\kappa^{(1)}, \quad G^{(2)} = EI^{(2)}\kappa^{(2)}, \quad H = \mu J\tau. \tag{2.7}$$

Here E is the Young's modulus and μ is the shear modulus of the material of the rod, $I^{(1)}$ and $I^{(2)}$ are the principal moments of inertia of the cross-section of the rod and μJ is the torsional rigidity of the cross-section of the rod. The equations (2.1)–(2.7) form the Kirchhoff–Love approximation in rod theory, in which warpage and shear effects are neglected.

Some kinematic relations are required to describe the centre line of the rod and the orientation of the cross-section at every point along it. These are most conveniently expressed in terms of the Euler angles, ψ, θ and ϕ, of the tangent to the centreline. The direction cosines with respect to the moving frame $\hat{l}$, $\hat{m}$ and $\hat{n}$, expressed in terms of those with respect to the fixed frame l, m and n, are (Love 1927, p. 385)

$$\begin{pmatrix} \hat{l} \\ \hat{m} \\ \hat{n} \end{pmatrix} = \begin{bmatrix} -S_\psi S_\phi + C_\psi C_\phi C_\theta & C_\psi S_\phi + S_\psi C_\phi C_\theta & -S_\theta C_\phi \\ -S_\psi C_\phi - C_\psi S_\phi C_\theta & C_\psi C_\phi - S_\psi S_\phi C_\theta & S_\theta S_\phi \\ S_\theta C_\psi & S_\theta S_\psi & C_\theta \end{bmatrix} \begin{pmatrix} l \\ m \\ n \end{pmatrix}. \tag{2.8}$$

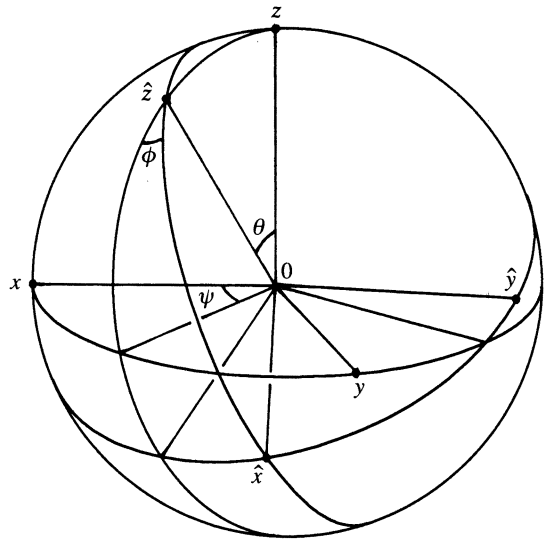

Figure 1. The Euler angles ψ, θ, and ϕ determine the orientation of the moving coordinate axes $\hat{x}$, $\hat{y}$, $\hat{z}$ relative to the fixed coordinate axes x, y, z. The tangent to the centreline of the rod is along $\hat{z}$, and the principal axes of the cross-section are along $\hat{x}$ and $\hat{y}$.

Here, $S_{(\cdot)} \equiv \sin(\cdot)$ and $C_{(\cdot)} \equiv \cos(\cdot)$. This determines the orientation of the cross-section at every point along the centre line as shown in figure 1. Then the coordinates of the centre line of the rod with respect to a fixed basis, x, y and z, satisfy the first-order ordinary differential equations (Love 1927, p. 413)

$$x_s = \sin\theta\cos\psi, \quad y_s = \sin\theta\sin\psi, \quad z_s = \cos\theta. \tag{2.9}$$

The Euler angles also enable us to write down the components of the curvature, and the twist of the centreline, which describe the strain in the rod as (Love 1927, p. 386)

$$\kappa^{(1)} = \theta_s\sin\phi - \psi_s\sin\theta\cos\phi, \quad \kappa^{(2)} = \theta_s\cos\phi + \psi_s\sin\theta\sin\phi, \quad \tau = \phi_s + \psi_s\cos\theta. \tag{2.10}$$

Upon substituting the expressions for $G^{(1)}$, $G^{(2)}$ and H from equation (2.7) into equations (2.4)–(2.6), we get six equations. Along with the equations (2.9) and (2.10), they form a system of 12 first-order ordinary differential equations for the twelve variables $\kappa^{(1)}$, $\kappa^{(2)}$, τ, $N^{(1)}$, $N^{(2)}$, T, ψ, θ, ϕ, x, y and z as functions of s.

To specify the boundary-value problem completely, we need 12 boundary conditions. Fixing the two ends of the rod at the origin of the fixed coordinate system gives six conditions. Aligning the moving frame at one end of the rod, $s = 0$, with the fixed axes results in three more conditions. Finally, by observing that the principal axes of the moving frame corresponding to the other end, $s = l$, have undergone a half-twist about the tangent to the centreline, we get another three conditions. By adopting a configuration that avoids the polar singularities of the Euler angles at $\theta = 0$ and $\theta = \pi$, we can write the boundary conditions as

$$\left.\begin{aligned} x(0) = 0, \quad x(l) = 0, \quad \psi(0) = 0, \quad \psi(l) = 2\pi, \\ y(0) = 0, \quad y(l) = 0, \quad \theta(0) = \tfrac{1}{2}\pi, \quad \theta(l) = \tfrac{1}{2}\pi, \\ z(0) = 0, \quad z(l) = 0, \quad \phi(0) = 0, \quad \phi(l) = \pi. \end{aligned}\right\} \tag{2.11}$$

This completes the formulation of the boundary-value problem for the equilibrium configuration of the rod.

3. Simplification

To facilitate analysis, we simplify the equations by eliminating some variables and scaling the rest to make them dimensionless. By using (2.4) and (2.5), we can eliminate $N^{(1)}$ and $N^{(2)}$ from equations (2.1)–(2.3). Next, we define the dimensionless variables

$$\left.\begin{gathered}\bar{s}=2\pi s/l, \quad \bar{x}=2\pi x/l, \quad \bar{y}=2\pi y/l, \quad \bar{z}=2\pi z/l,\\ \bar{\kappa}^{(1)}=\kappa^{(1)}l/2\pi, \quad \bar{\kappa}^{(2)}=\kappa^{(2)}l/2\pi, \quad \bar{\tau}=\tau l/2\pi, \quad t=Tl^2/4\pi^2\mu J,\\ \alpha=EI^{(1)}/\mu J, \quad \beta=EI^{(2)}/\mu J.\end{gathered}\right\} \tag{3.1}$$

Then the twelfth-order system of equations for the variables $\kappa^{(1)}$, $\kappa^{(2)}$, τ, t, ψ, θ, ϕ, x, y and z becomes, upon dropping the bars for convenience,

$$\left.\begin{aligned}\alpha\kappa^{(1)}_{ss} &= -(1-\beta)(\tau\kappa^{(2)})_s+(\alpha-1)\tau^2\kappa^{(1)}+\beta\tau\kappa^{(2)}_s+t\kappa^{(1)},\\ \beta\kappa^{(2)}_{ss} &= (1-\alpha)(\tau\kappa^{(1)})_s+(\beta-1)\tau^2\kappa^{(2)}-\alpha\tau\kappa^{(1)}_s+t\kappa^{(2)},\\ \tau_s &= (\alpha-\beta)\kappa^{(1)}\kappa^{(2)},\\ t_s &= -\alpha\kappa^{(1)}\kappa^{(1)}_s-\beta\kappa^{(2)}\kappa^{(2)}_s-(\alpha-\beta)\kappa^{(1)}\kappa^{(2)}\tau,\\ \psi_s &= (-\kappa^{(1)}\cos\phi+\kappa^{(2)}\sin\phi)/\sin\theta,\\ \theta_s &= \kappa^{(1)}\sin\phi+\kappa^{(2)}\cos\phi,\\ \phi_s &= (\kappa^{(1)}\cos\phi-\kappa^{(2)}\sin\phi)/\tan\theta+\tau,\\ x_s &= \sin\theta\cos\psi,\\ y_s &= \sin\theta\sin\psi,\\ z_s &= \cos\theta.\end{aligned}\right\} \tag{3.2}$$

Observation of a model of the Möbius band shows that it has a two-fold symmetry about an axis joining two points on the centreline. These points have a dimensionless arc-length separation of π and have the minimum spatial distance between them. Choosing them to be $s=0$ and $s=\pi$, we need consider only the domain $[0,\pi]$ for the purposes of analysis. Then, the boundary conditions for the dimensionless variables at the points $s=0$ and $s=\pi$ are

$$\left.\begin{array}{llll} x(0)=0, & y(0)=0, & x(\pi)=0, & z(\pi)=0,\\ z(0)=0, & \psi(0)=0, & \psi(\pi)=\pi, & \phi(\pi)=\tfrac{1}{2}\pi,\\ \theta(0)=\tfrac{1}{2}\pi, & \phi(0)=0, & \kappa^{(1)}(\pi)=0, & \kappa^{(2)}_s(\pi)=0.\end{array}\right\} \tag{3.3}$$

The equations (3.2) together with the boundary conditions (3.3) constitute a nonlinear two-point boundary-value problem.

Before outlining the solution procedure, we pause to consider some facts about a physical model of the Möbius strip made of a thin sheet of paper. For a rod with a rectangular cross-section of width $2a$ and height $2b$, the flexural and torsional rigidities are (Love 1927, p. 324)

$$\left.\begin{gathered}EI^{(1)}=\tfrac{4}{3}Ea^3b, \quad EI^{(2)}=\tfrac{4}{3}Eb^3a,\\ \mu J\approx\mu ab^3(16/3-3.361b/a), \quad a/b\gg 1.\end{gathered}\right\} \tag{3.4}$$

In fact, the expression for μJ is very accurate for $a/b>3$.

Therefore, the ridigity ratios α and β defined in (3.1) are given by

$$\alpha=\frac{8(1+\nu)a^2}{3b^2(16/3-3.361b/a)}, \quad \beta=\frac{8(1+\nu)}{3(16/3-3.361b/a)}, \tag{3.5}$$

where $\nu = (E/2\mu) - 1$ is Poisson's ratio.

Typically $a/b \approx 500$ for a sheet of paper or plastic. Hence,

$$\alpha \approx 10^5(1+\nu), \quad \beta \approx 0.5(1+\nu). \tag{3.6}$$

Since Poisson's ratio ν, lies in the range $0 \leqslant \nu \leqslant 0.5$ for ordinary materials, (3.6) shows that the dimensionless rigidity β, lies in the range $0.5 \leqslant \beta \leqslant 0.75$. We shall calculate the solution only for the extreme values of this range, namely $\beta = 0.5$ and $\beta = 0.75$. However, as (3.6) shows, we must consider large values of α.

4. Method of solution

For a rod with a square cross-section, we have $a = b$, so that $\alpha = \beta$. Then an exact solution of the boundary-value problem (3.2) and (3.3) is given by

$$\left.\begin{gathered} x_0(s) = \sin s, \quad y_0(s) = 1 - \cos s, \quad z_0(s) = 0, \quad \theta_0(s) = \tfrac{1}{2}\pi, \\ \psi_0(s) = s, \quad \phi_0(s) = \tfrac{1}{2}s \quad \kappa_0^{(1)}(s) = -\cos(\tfrac{1}{2}s), \quad \kappa_0^{(2)}(s) = \sin(\tfrac{1}{2}s) \\ \tau_0(s) = \tfrac{1}{2}, \quad t_0(s) = 0. \end{gathered}\right\} \tag{4.1}$$

This solution corresponds to a very narrow Möbius band with a circular centre line of unit radius and centre at $(0, 1, 0)$, lying in the xy plane.

When the symmetry $\alpha = \beta$ is broken, so that $\alpha > \beta$, the rod no longer stays in the plane. Instead, it assumes the shape of a space curve with torsion different from zero. Of course when $\alpha - \beta \ll 1$, this space curve is very nearly circular. We exploit this fact by using the circular solution (4.1) as the initial guess in an iterative procedure to solve the boundary-value problem for $\alpha = \beta + \delta$, where δ is a small quantity. Once the solution for $\alpha = \beta + \delta$ has been found, we use it as the initial guess to find the solution for $\alpha = \beta + 2\delta$, and so on. This procedure constitutes a continuation method or homotopy method with α as the continuation parameter.

At each step of the continuation scheme, we use COLSYS (Ascher *et al.* 1983), a numerical boundary-value problem solver, to compute the solution. It uses spline collocation at gaussian points. A brief description of the method is as follows: a nonlinear system of equations for the unknown B-spline coefficients is obtained by forcing a collocation solution to satisfy the boundary conditions and the differential equations at the Gauss–Legendre points in a previously defined mesh. A damped quasi-Newton method is used to solve the nonlinear system iteratively, with a starting guess as the first iterate. *A posteriori* error estimates are then used to refine the mesh adaptively until the specified tolerances are met. The coefficients of the collocation solution are stored to allow for the possibility of simple continuation. In the absence of bifurcation and turning or fold points, as in our case, the continuation algorithm simply involves solving a sequence of nonlinear problems. Then each solution gives an initial approximation to the solution at the next step.

To follow the continuation path, we start with the exact solution for $\alpha = \beta = 0.5$ or $\alpha = \beta = 0.75$ and increase α in steps of 0.1, solving a nonlinear problem at each step. As α becomes larger, we increase the step size. On a uniform mesh with 40 subintervals, the quasi-Newton method takes two iterations per continuation step when the error tolerances on the coordinates x, y and z are 10^{-4}.

Figure 2*a–c* shows the orthographic projections of the rod solution on the three coordinate planes for $\beta = 0.5$ and $\alpha = 0.5$, 1, 5, 10 and 50 respectively. They trace the evolution of the shape of the centre line of a band of given thickness as a function of its width. Comparisons of the results show good agreement with physical Möbius

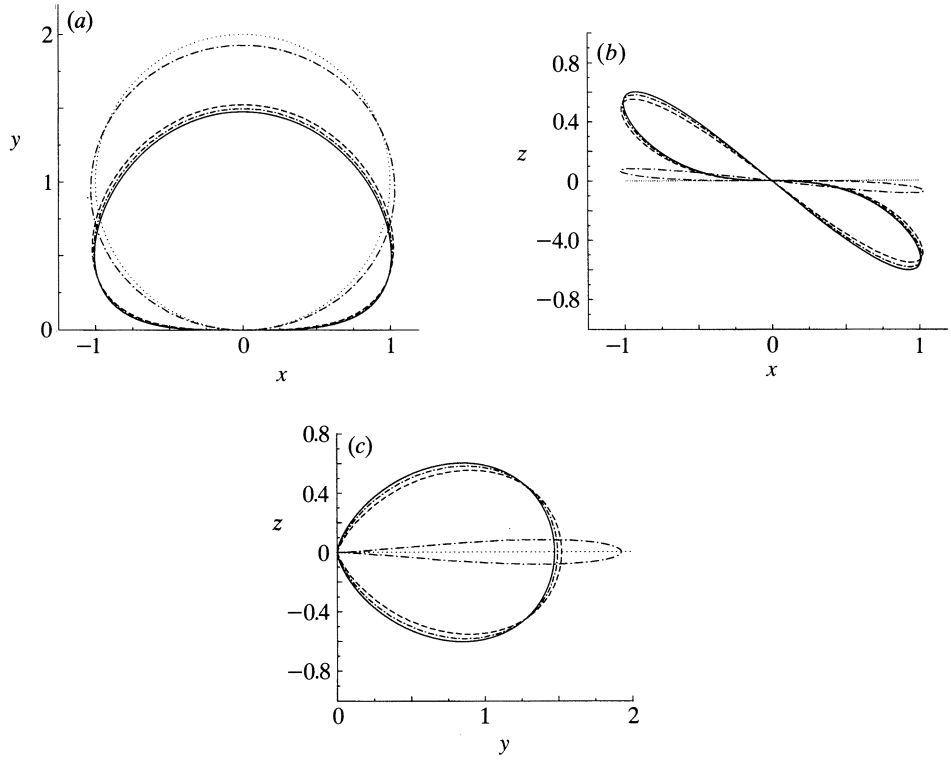

Figure 2. The projections of the centreline of the rod on the three coordinate planes for $\beta = 0.5$ and $\alpha = 0.5$ (·····), 1 (—·—), 5 (———), 10 (–·–) and 50 (———). (*a*) Projection on the xy plane. (*b*) Projection on the xz plane. (*c*) Projection on the yz plane.

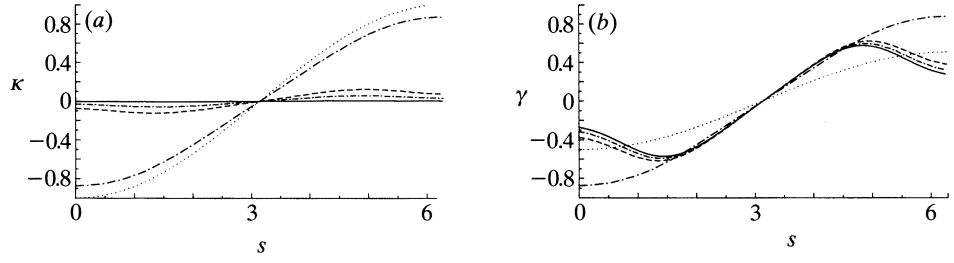

Figure 3. (*a*) The curvature $\kappa^{(1)}(s)$ and (*b*) the corresponding flexural couple $\gamma(s) = \alpha\kappa^{(1)}(s)$ for $\beta = 0.5$ and the same six values of α as in figure 2, i.e. $\alpha = 0.5$ (·····), 1 (—·—), 5 (———), 10 (–·–) and 50 (———).

bands of various widths; wider Möbius bands are further out of the plane than narrower ones and approach a limiting shape. Figure 3*a*, *b* shows the corresponding values of the curvature $\kappa^{(1)}(s)$, and the flexural couple $\gamma(s) = \alpha\kappa^{(1)}(s)$, for $\beta = 0.5$ and the same values of α.

The curves in figures 2 and 3 indicate that the shape of the centreline of the Möbius band, its curvature in the stiff direction $\kappa^{(1)}(s)$, and the corresponding flexural couple $\gamma(s)$, all converge to limiting values as $\alpha \to \infty$. The limiting value of $\kappa^{(1)}(s)$ in figure 3*a* appears to be $\kappa^{(1)}(s) = 0$, while figure 3*b* shows that $\gamma(s) = \alpha\kappa^{(1)}(s)$ tends to a finite non-zero limit. In view of these numerical results, we shall seek an asymptotic solution of (3.2) and (3.3) for $\alpha \gg 1$.

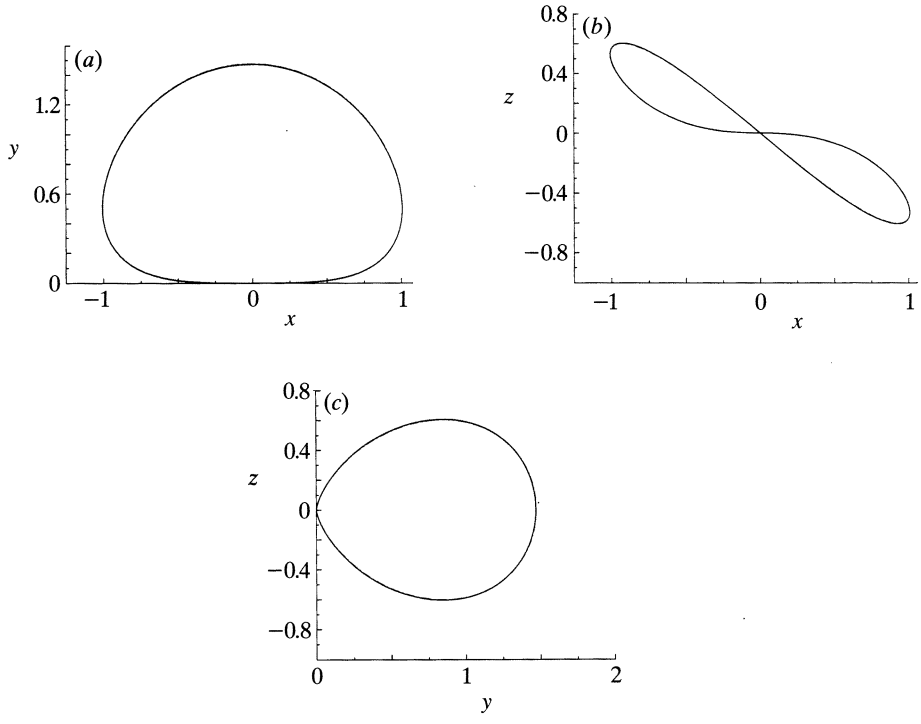

Figure 4. The projections of the asymptotic solution for $\alpha \gg 1$ on the three coordinate planes for $\beta = 0.5$ (——). The projections of the solution to the exact equations for $\alpha = 50$ (— · —) and $\beta = 0.5$ are shown for comparison, but they are almost indistinguishable from the exact solution. (*a*) xy plane. (*b*) xz plane. (*c*) yz plane.

5. Asymptotic solution for $\alpha \gg 1$

We assume that for large α, the asymptotic form of $\kappa^{(1)}(s,\alpha)$ is $\gamma(s)/\alpha$ and that the asymptotic form of all other unknowns is independent of α. Thus

$$\left.\begin{aligned} \kappa^{(1)}(s,\alpha) \sim \alpha^{-1}\gamma(s), \quad \kappa^{(2)}(s,\alpha) \sim \kappa^{(2)}_\infty(s), \quad \tau(s,\alpha) \sim \tau_\infty(s), \quad t(s,\alpha) \sim t_\infty(s), \\ \psi(s,\alpha) \sim \psi_\infty(s), \quad \theta(s,\alpha) \sim \theta_\infty(s), \quad \phi(s,\alpha) \sim \phi_\infty(s), \quad x(s,\alpha) \sim x_\infty(s), \\ y(s,\alpha) \sim y_\infty(s), \quad z(s,\alpha) \sim z_\infty(s). \end{aligned}\right\} \tag{5.1}$$

We substitute (5.1) into (3.2) and equate the coefficients of α^0, which are the terms of highest order. Then, upon dropping the subscripts, we get the equations

$$\left.\begin{aligned} \gamma_{ss} = (\beta-1)(\tau\kappa^{(2)})_s + \gamma\tau^2 + \beta\tau\kappa^{(2)}_s, \\ \beta\kappa^{(2)}_{ss} = -2\gamma_s\tau + (\beta-1)\tau^2\kappa^{(2)} - \gamma\tau_s + t\kappa^{(2)}, \quad \tau_s = \gamma\kappa^{(2)}, \\ t_s = -\beta\kappa^{(2)}_s\kappa^{(2)} - \gamma\kappa^{(2)}\tau, \quad \psi_s = \kappa^{(2)}\sin\phi/\sin\theta, \\ \theta_s = \kappa^{(2)}\cos\phi, \quad \phi_s = -\kappa^{(2)}\sin\phi/\tan\theta + \tau, \\ x_s = \sin\theta\cos\psi, \quad y_s = \sin\theta\sin\psi, \quad z_s = \cos\theta. \end{aligned}\right\} \tag{5.2}$$

These equations are just the limiting forms of (3.2) as $\alpha \to \infty$. Equations (5.2) along with the boundary conditions (3.3), with $\gamma(\pi) = 0$ instead of $\kappa^{(1)}(\pi) = 0$, constitute the boundary-value problem for the asymptotic solution.

To solve (5.2) and (3.3) numerically we use the same continuation procedure used to solve (3.2) and (3.3). The configuration (4.1), with $\gamma_0(s) = -\beta\cos s/2$ instead of

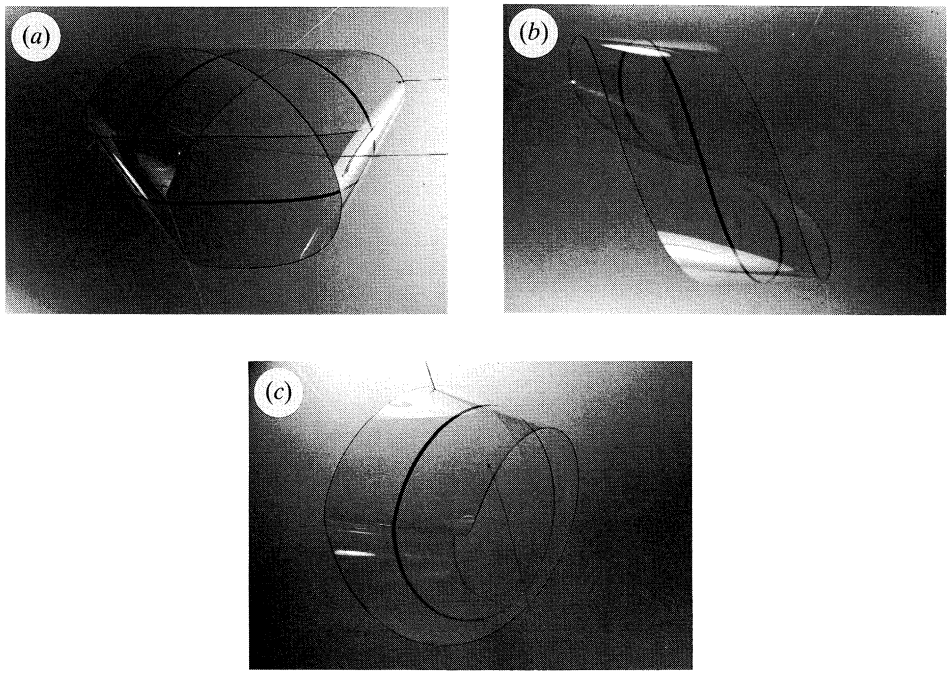

Figure 5. Photographs of a Möbius band made of plastic when viewed along the three coordinate axes. The centreline is shown as a dark line. The photographs correspond to the projections on the (*a*) *xy* plane, (*b*) *xz* plane, (*c*) *yz* plane and should be compared with the corresponding projections of the computed solution shown in figure 4.

$\kappa_0^{(1)}(s) = -\cos s/2$, suffices as an initial guess for the iteration scheme. On a uniform mesh of 40 subintervals, and an error tolerance of 10^{-4} on the coordinates x, y and z, the quasi-Newton method implemented in COLSYS takes six iterations to converge to the asymptotic solution.

Figure 4*a–c* shows the projections of the asymptotic solution for $\beta = 0.5$ on the three coordinate planes. For comparison, the numerical solution of the exact equations (3.2) and (3.3) with $\beta = 0.5$ and $\alpha = 50$ is also shown. We observe that the asymptotic solution and the solution to the exact equations are indistinguishable to graphical accuracy.

Three photographs of a Möbius band constructed from a sheet of plastic are shown in figure 5(*a–c*). The centreline is shown as a dark line. The projections of this line as shown in the photographs, are very similar to the computed results shown in figure 4*a–c*.

6. Energy

The energy stored in a bent and twisted rod is given in terms of its curvature, twist, and by elastic

$$U = \int_0^l \tfrac{1}{2}[EI^{(1)}(\kappa^{(1)}(s))^2 + EI^{(2)}(\kappa^{(2)}(s))^2 + \mu J\tau^2(s)]\,\mathrm{d}s. \tag{6.1}$$

Using the variables, $\bar{s}, \bar{\kappa}^{(1)}, \bar{\kappa}^{(2)}$, α and β, we may write

$$U = (2\pi\mu J/l)\,U_{\mathrm{d}}. \tag{6.2}$$

On dropping the bars the dimensionless energy is

$$U_{\mathrm{d}} = \int_0^{2\pi} \tfrac{1}{2}[\alpha(\kappa^{(1)}(s))^2 + \beta(\kappa^{(2)}(s))^2 + \tau^2(s)]\,\mathrm{d}s. \tag{6.3}$$

To compute this integral, we make use of the existence of a conserved quantity. From the third and fourth equations of (3.2), it follows that

$$t_s + \alpha\kappa^{(1)}\kappa_s^{(1)} + \beta\kappa^{(2)}\kappa_s^{(2)} + \tau\tau_s = 0. \tag{6.4}$$

On integrating, we get

$$t(s) + \tfrac{1}{2}[\alpha(\kappa^{(1)}(s))^2 + \beta(\kappa^{(2)}(s))^2 + \tau^2(s)] = H = \text{const.} \tag{6.5}$$

Here H is the equivalent of the energy of a free rigid body in the kinetic analogy due to Kirchhoff (Love 1927, §260).

Integrating (6.5) over the dimensionless length of the rod gives

$$\int_0^{2\pi} [t + \tfrac{1}{2}\alpha(\kappa^{(1)})^2 + \tfrac{1}{2}\beta(\kappa^{(2)})^2 + \tfrac{1}{2}\tau^2]\,\mathrm{d}s = 2\pi H. \tag{6.6}$$

For a closed self-equilibrated rod,

$$\int_0^{2\pi} t(s)\,\mathrm{d}s = 0, \tag{6.7}$$

so that

$$U_{\mathrm{d}} = \int_0^{2\pi} \tfrac{1}{2}[\alpha(\kappa^{(1)})^2 + \tfrac{1}{2}\beta(\kappa^{(2)})^2 + \tfrac{1}{2}\tau^2]\,\mathrm{d}s = 2\pi H. \tag{6.8}$$

In the asymptotic limit $\alpha \gg 1, \kappa^{(1)} \sim 0$, the energy is

$$U_{\mathrm{d}} \sim \int_0^{2\pi} \tfrac{1}{2}[\beta(\kappa^{(2)})^2 + \tau^2]\,\mathrm{d}s \equiv 2\pi H_{\mathrm{asym}}. \tag{6.9}$$

The numerical solution computed in §5 yields $H_{\mathrm{asym}} = 0.6256$ for $\nu = 0$, and $H_{\mathrm{asym}} = 0.7997$ for $\nu = 0.5$. Therefore, using the expression from (3.4) for μJ when $a \gg b$, we calculate the energy of the rod for $\nu = 0$ to be

$$U = (\mu ab^3/l)\,13.35\pi^2 = (Eab^3/l)\,6.67\pi^2, \tag{6.10}$$

and for $\nu = 0.5$ to be

$$U = (\mu ab^3/l)\,17.06\pi^2 = (Eab^3/l)\,5.69\pi^2. \tag{6.11}$$

This completes our analysis of the rod model of a Möbius band, and we now consider the shell model.

7. Thin inextensible shells

A Möbius band made from a flat strip of paper may be viewed as a thin elastic shell in equilibrium with no external forces acting on it. Since paper is almost inextensible, the elastic energy of deformation is due to bending alone. It can be written as $4\pi ab^3E[3(1-\nu^2)\,l]^{-1}V$, where the dimensionless energy V is given by

$$V = \frac{l}{4\pi a}\int_0^l \int_{-a}^{a} \hat{\kappa}^2(u, s)\,\mathrm{d}u\,\mathrm{d}s. \tag{7.1}$$

Here E is the Young's modulus for paper, $2b$ is the thickness of the paper, l is the length of the strip, $2a$ is its width, and $\hat{\kappa}(u, s)$ is the mean curvature of the middle surface of the band. The equilibrium configuration of the band is determined by the requirement that V be stationary with respect to small inextensible variations. The shape will be stable if V is a local minimum in this space of variations.

Since the band is a developable surface, it is completely determined by its centreline and the generators of the surface at every point along it. Let the angle between the generator and the tangent to the centreline at the point s along it be denoted by $\xi(s)$. Then the two-dimensional integral (7.1) can be reduced to a one-dimensional integral along the centreline and rewritten as (Wunderlich 1963).

$$V = \frac{l}{4\pi a}\int_0^l \frac{[\kappa^2(s)+\omega^2(s)]^2}{\kappa^2(s)}\frac{\sin^2\xi}{\xi_s}\ln\left[\frac{\sin^2\xi+a\xi_s}{\sin^2\xi-a\xi_s}\right]\mathrm{d}s. \tag{7.2}$$

Here $\kappa(s)$ and $\omega(s)$ are the curvature and torsion of the centreline of the band, and $\xi(s)$ is related to them by

$$\xi(s) = \arctan\left(\kappa(s)/\omega(s)\right). \tag{7.3}$$

It is convenient to use the dimensionless variables $\bar{s} = 2\pi s/l$, $\bar{\kappa} = \kappa l/2\pi$ and $\bar{\omega} = \omega l/2\pi$ to rewrite (7.2), with overbars omitted, in the following form:

$$V = \frac{l}{4\pi a}\int_0^{2\pi} \frac{[\kappa^2(s)+\omega^2(s)]^2}{\kappa^2(s)}\frac{\sin^2\xi}{\xi_s}\ln\left[\frac{\sin^2\xi+2\pi a l^{-1}\xi_s}{\sin^2\xi-2\pi a l^{-1}\xi_s}\right]\mathrm{d}s. \tag{7.4}$$

It is necessary that $\xi(s)$ satisfy the condition

$$|\sin^2\xi(s)| > 2\pi a l^{-1}|\xi_s(s)| \tag{7.5}$$

to preclude the possibility that the generators intersect each other within the band. The variational problem consists of finding the middle curve that makes V, given by (7.4), stationary among all closed curves of length l for which the corresponding band has one half-twist.

The absolute value of the factor

$$\xi_s^{-1}\sin^2\xi\ln\left[(\sin^2\xi+2\pi a l^{-1}\xi_s)(\sin^2\xi-2\pi a l^{-1}\xi_s)^{-1}\right]$$

in the integrand in (7.4) is greater than or equal to $4\pi a l^{-1}$. Therefore,

$$V \geqslant \int_0^{2\pi}\frac{[\kappa^2(s)+\omega^2(s)]^2}{\kappa^2(s)}\mathrm{d}s \equiv V_n. \tag{7.6}$$

In fact, V_n is the asymptotic form of the energy for small a/l, i.e. for a narrow band. Sadowsky (1930) constructed a developable surface with one half-twist, not in equilibrium, for which $V_n = 7.5\pi$. Later Wunderlich (1963) constructed one, also not in equilibrium, for which $V_n = 6.763\pi$. Therefore, the dimensionless energy of a narrow Möbius band at equilibrium V_n^e, satisfies

$$V_n^e \leqslant 6.763\pi. \tag{7.7}$$

We shall obtain a smaller upper bound on V_n^e. To do so, we consider the centreline of the rod as given by the asymptotic solution in §5. The dimensionless curvature and torsion of the centreline, $\kappa(s)$ and $\omega(s)$ respectively, are

$$\kappa(s) = \kappa^{(2)}(s), \quad \omega(s) = \tau(s). \tag{7.8}$$

Here, $\kappa^{(2)}(s)$ and $\tau(s)$ are the curvature and twist of the centreline corresponding to

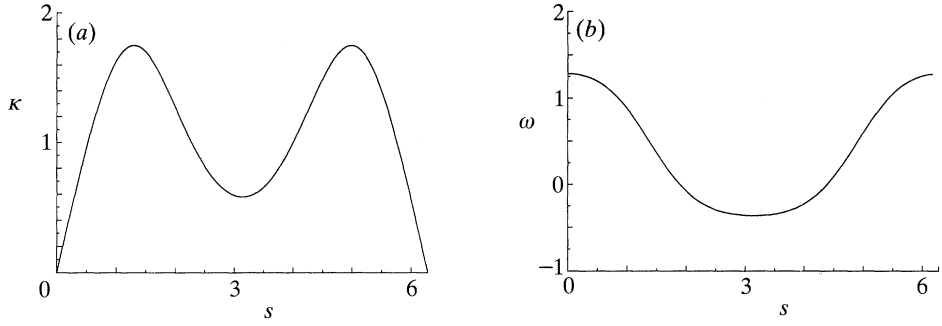

Figure 6. (*a*) The curvature $\kappa(s)$ and (*b*) the torsion $\omega(s)$, of the centreline corresponding to the asymptotic solution with $\alpha \gg 1$ and $\beta = 0.5$.

the asymptotic solution (see Appendix A). Figure 6 shows the curvature and torsion of the centreline for the Poisson's ratio $\nu = 0$, i.e. $\beta = 0.5$. We observe that at $s = 0$ and $s = 2\pi$, the curvature vanishes but the torsion is non-zero. Near these two points $\xi(s)$, given by (7.3), is very small while $\xi_s(s) = (\kappa^2 + \omega^2)^{-1}(\kappa_s \omega - \omega_s \kappa)$ is moderately large. Therefore the inequality (7.5) is not satisfied in the domains where the generators intersect within the band, namely $[0, s_0]$ and $[2\pi - s_0, 2\pi]$. Here s_0 is given by the solution of the equation

$$\sin^2 \xi(s_0) = (2\pi a/l)\, \xi_s(s_0). \tag{7.9}$$

In fact this is the condition for neighbouring generators at a point s_0 along the centreline to intersect at the edge of the band of width $2a$.

To allow for the construction of a continuous closed developable surface, we replace the centreline computed in §5 by a 'helix' in the domains $[0, s_0]$ and $[2\pi - s_0, 2\pi]$. This curve is assumed to have a linearly varying curvature and a linearly varying torsion and is determined by the equations

$$\kappa(s) = \begin{cases} \kappa(s_0)\, s/s_0, & s \in [0, s_0] \\ \kappa(2\pi - s_0)\, s/(2\pi - s_0), & s \in [2\pi - s_0, 2\pi], \end{cases} \tag{7.10}$$

$$\omega(s) = \begin{cases} \omega(s_0)\, s/s_0, & s \in [0, s_0] \\ \omega(2\pi - s_0)\, s/(2\pi - s_0), & s \in [2\pi - s_0, 2\pi]. \end{cases} \tag{7.11}$$

The generators of the associated developable make a constant angle $\xi(s) = \arctan(\kappa(s_0)/\omega(s_0))$ with the tangent to the centreline and do not intersect each other anywhere. When patched together with the existing developable surface on the domain $[s_0, 2\pi - s_0]$, it yields a surface with one half-twist that we expect to be a good approximation to the actual Möbius band.

Next, we rewrite the dimensionless energy of a narrow Möbius band, given by (7.6), as

$$V_n = V_n^1 + V_n^2, \tag{7.12}$$

where

$$V_n^1 = \int_{s_0}^{2\pi - s_0} \frac{[\kappa^2(s) + \omega^2(s)]^2}{\kappa^2(s)}\, \mathrm{d}s, \tag{7.13}$$

$$V_n^2 = 2 \int_0^{s_0} \frac{[\kappa^2(s) + \omega^2(s)]^2}{\kappa^2(s)}\, \mathrm{d}s. \tag{7.14}$$

Table 1. *The energies V and V_n, corresponding to the asymptotic solution for $\nu = 0$*

a/l	s_0	$\kappa(s_0)$	$\omega(s_0)$	V	V_n
0.05	0.5027	0.9615	1.1939	5.20π	4.95π
0.10	0.6912	1.3287	1.1261	4.69π	4.23π
0.15	0.8796	1.5240	0.9382	4.24π	3.63π

Table 2. *The energies V and V_n, corresponding to the asymptotic solution for $\nu = 0.5$*

a/l	s_0	$\kappa(s_0)$	$\omega(s_0)$	V	V_n
0.05	0.5027	1.0440	1.2857	5.08π	4.79π
0.10	0.6912	1.3287	1.1261	4.41π	3.92π
0.15	0.8796	1.5240	0.9382	4.07π	3.26π

Both integrals depend on s_0; V_n^1 is the energy of the surface whose centreline is given by the asymptotic solution and V_n^2 is the energy of the surface associated with the curve given by (7.10) and (7.11). To find s_0, we first evaluate $\xi(s)$ for the centreline of the asymptotic solution using (7.3). Then we solve (7.9) numerically for s_0, and find $\kappa(s_0)$ and $\omega(s_0)$ using (7.8). We evaluate V_n^1 numerically as a Riemann sum, and V_n^2 analytically by substituting (7.10) and (7.11) into (7.6). Finally, we use (7.12) to compute V_n.

Similarly, the dimensionless energy of a wide Möbius band, given by (7.4), is written as a sum of integrals over the domains $[s_0, 2\pi - s_0]$ and $[0, s_0]$ and evaluated by following an identical procedure. In table 1, we show V_n and V for some values of a/l, using the asymptotic solution when the Poisson's ratio $\nu = 0$. In table 2, the corresponding values are shown when $\nu = 0.5$.

We note that $V > V_n$ as (7.6) shows, and as a/l is decreased, V approaches V_n. Furthermore, V_n is much less than the bound given by (7.7). The energy V shown in tables 1 and 2 is an upper bound on the actual energy of an equilibrated Möbius band of given a/l, and is probably close to it.

Finally we compare the upper bound $Eab^3 l^{-1}[4V/3\pi(1-\nu^2)]$ on the energy of the shell with the energy U of the rod, expressing each in units of $\pi^2 Eab^3 l^{-1}$. For the narrowest band listed in table 1 we have $a/l = 0.05$, $\nu = 0$ and $V = 5.20\pi$ so the energy is $4(5.20)/3 = 6.93$, while for the rod with $\nu = 0$, (6.10) yields 6.67. Thus for $\nu = 0$ the shell energy is just 4% greater than the rod energy. The corresponding energies for $\nu = 0.5$ are 9.03 for the shell (from table 2) and 5.96 for the rod (from (6.11)). This discrepancy is a consequence of the different hypotheses underlying the two theories, which difference is unimportant when $\nu = 0$.

Appendix A. The curvature and torsion of the centreline

The equations of equilibrium for a rod, as presented in §2, are valid in a frame of reference that is convected along the centreline. The structure of the cross-section of the rod makes it most convenient to choose a frame that consists of the principal axes of the cross-section and the tangent to the centreline of the rod. This frame, which we shall call the rod frame, is in general, not the same as the Frenet frame consisting of the normal, the binormal and the tangent associated with the centreline. Therefore the curvature components and the twist as measured in the rod frame are not the same as the curvature and torsion as measured in the Frenet frame.

The curvature of the centreline $\kappa(s)$ is given by

$$\kappa(s) = [(\kappa^{(1)}(s))^2 + (\kappa^{(2)}(s))^2]^{\frac{1}{2}}. \tag{A 1}$$

Here $\kappa^{(1)}(s)$ and $\kappa^{(2)}(s)$, given by the first two equations in (2.10), are the components of the curvature in the rod frame. Also, the torsion of the centreline $\omega(s)$ differs from the twist $\tau(s)$ given by the third equation in (2.10). This may be seen easily in a simple example: a thin wire that is twisted and straight has twist but no torsion.

In the asymptotic case, $\kappa^{(1)}(s) \sim 0$. From (A 1) it follows that $\kappa(s) = \kappa^{(2)}(s)$. Thus the curvature vector lies along the $\kappa^{(2)}$ principal axis, which is coincident with the binormal. Then the rod frame and the Frenet frame are coincident everywhere along the centreline. As a consequence the twist of the centreline is identical with its torsion, thus justifying (7.8).

Appendix B. A lower bound on V_n

We shall derive a crude lower bound on the dimensionless energy of a narrow Möbius band. For a non self-intersecting smooth closed space curve with curvature $\kappa(s)$, projected onto a fixed plane oriented so that the projection has no self intersections

$$\kappa_p(s) = \kappa(s)\cos\eta(s). \tag{B 1}$$

Here $\kappa_p(s)$ is the curvature of the planar projection of the space curve and $\eta(s)$ is the angle that the osculating plane to the curve makes with the given plane. For a smooth planar closed curve with curvature $\kappa_p(s)$ without any self-intersections

$$\int_0^{2\pi} \kappa_p(s)\,\mathrm{d}s = 2\pi. \tag{B 2}$$

Upon substituting (B 1) into (B 2), we get

$$\int_0^{2\pi} \kappa(s)\cos\eta(s)\,\mathrm{d}s = 2\pi. \tag{B 3}$$

Since $\kappa(s) \geqslant 0$ and $|\cos\eta(s)| \leqslant 1$, we have

$$\int_0^{2\pi} \kappa(s)\,\mathrm{d}s \geqslant 2\pi. \tag{B 4}$$

Therefore, using (B 4), we get

$$\begin{aligned}\int_0^{2\pi} \kappa^2(s)\,\mathrm{d}s &= \int_0^{2\pi} [(\kappa(s)-1)^2 + 2\kappa(s) - 1]\,\mathrm{d}s \\ &\geqslant \int_0^{2\pi} [\kappa(s)-1]^2 + 2\pi \\ &\geqslant 2\pi. \end{aligned} \tag{B 5}$$

Finally use (B 5) in (7.6) to get

$$V_n \geqslant \int_0^{2\pi} \kappa^2(s)\,\mathrm{d}s \geqslant 2\pi. \tag{B 6}$$

This provides a lower bound on V_n.

References

Ascher, U., Christiansen, J. & Russell, R. D. 1983 COLSYS software for boundary value problems. *A.C.M. Trans Math. Software* **7**, 209–222.

Love, A. E. H. 1927 *A treatise on the mathematical theory of elasticity*, 4th edn. New York: Dover.

Sadowsky, M. 1930 Thëorie der elastisch biegsamen undehnbaren Bänder mit Anwendungen auf das Möbius'sche band. *Proc. Int. Cong. appl. Mech., Stockholm* **2**, 444–451.

Schwarz, G. E. 1990 The dark side of the Moebius strip. *Am. Math. Monthly* **97**, 890–897.

Wunderlich, W. 1963 Über ein abwickelbares Möbiusband. *Monat. Math.* **66**, 276–289.

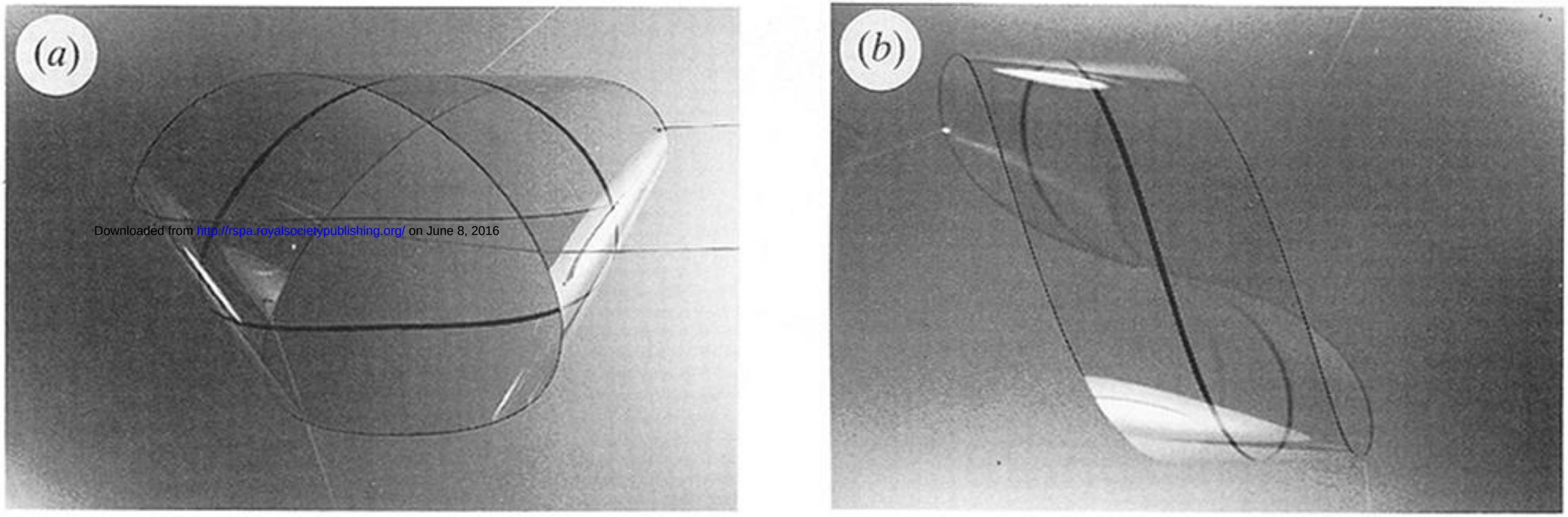

Figure 5. Photographs of a Möbius band made of plastic when viewed along the three coordinate axes. The centreline is shown as a dark line. The photographs correspond to the projections on the (*a*) *xy* plane, (*b*) *xz* plane, (*c*) *yz* plane and should be compared with the corresponding projections of the computed solution shown in figure 4.